

## Separation efficiency of a hydrodynamic separator using a 3D CFD approach

### Modélisation 3D multi-échelle du transport particulaire dans un séparateur hydrodynamique

Vivien Schmitt<sup>1</sup>, Matthieu Dufresne<sup>1</sup>, José Vazquez<sup>1</sup>, Martin Fischer<sup>1</sup>, Antoine Morin<sup>2</sup>

<sup>1</sup>Ecole Nationale du Génie de l'Eau et de l'Environnement de Strasbourg,  
Institut de Mécanique des Fluides et des Solides de Strasbourg

2 rue Boussingault, 67000 Strasbourg, France

[vivien.schmitt@engees.unistra.fr](mailto:vivien.schmitt@engees.unistra.fr)

<sup>2</sup>Hydroconcept, 46 avenue des frères Lumière, 78190 Trappes, France

## RÉSUMÉ

L'objectif de l'étude est d'investiguer l'utilisation des outils de modélisation 3D pour évaluer l'efficacité d'un séparateur hydrodynamique. La difficulté rencontrée consiste à modéliser aussi bien le comportement hydrodynamique global de l'ouvrage que les phénomènes locaux se produisant à proximité de la grille de séparation. Dans ce contexte, le développement d'une méthodologie multi-échelle a permis d'étudier l'ouvrage à différentes échelles (un modèle local représentant une portion de grille et un modèle global de l'ouvrage utilisant une grille conceptuelle de type milieu poreux). Cette approche a permis de diminuer considérablement le nombre de mailles et donc le temps de calcul. L'utilisation d'une approche euléro-lagrangienne a été utilisée pour suivre la trajectoire des particules au sein des deux modèles. Le modèle à l'échelle de l'ouvrage a mis en valeur l'influence des caractéristiques des particules sur la capacité de l'ouvrage à retenir des matières en suspension. L'augmentation de la masse volumique et du diamètre des particules favorise la sédimentation. Les particules de faibles densités sont quant à elles pilotées par l'hydrodynamique et potentiellement retenues par l'ouvrage. L'utilisation du modèle à l'échelle de la grille a permis de visualiser la trajectoire des particules à proximité de la grille. La comparaison entre deux types de grille (métal déployé et tôle perforée) a montré l'influence de la forme de la grille sur les effets d'énergie cinétique turbulente, phénomènes favorisant l'éjection des particules. Les résultats obtenus sont très prometteurs dans le cadre des techniques de séparation à l'aide d'une grille.

## ABSTRACT

The aim of this study is to investigate the use of Computational Fluid Dynamics (CFD) to predict the solid separation efficiency of a hydrodynamic separator. The numerical difficulty concerns the discretization of the geometry to simulate both the global behaviour and the local phenomena that occur nearby the screen. In this context, a CFD multiscale approach was developed: a global model (at the scale of the device) is used to visualize the hydrodynamic behaviour within the device; a local model (portion of the screen) is used to determine the local phenomena that occur nearby the screen. This approach allows us to minimize the number of cells and consequently to decrease the calculation time. The Eulerian-Lagrangian approach was used to model the particle trajectories in both models. Concerning the results, the global model shows the influence of the particles characteristics on the trapping efficiency. A high density favours the sedimentation. On the contrary, particles with small densities (1040 kg/m<sup>3</sup>) are steered by the hydrodynamic behaviour and can potentially be trapped by the separator. The use of the local model allows us to visualize the particles trajectories nearby the screen. A comparison between two types of screens (perforated plate vs. expanded metal) highlights the effects created by the shape of the screen. The turbulent kinetic energy observed near the apertures favours the ejection of the particles in this region. The results are promising about screening separation technics.

## KEYWORDS

3D CFD, Hydrodynamic separator, Multiscale approach, Particle tracking, Screen separation

## 1 INTRODUCTION

A significant part of pollutants is fixed on sediments and particles (Chebbo, 1992; Chocat, 1997; Ashley et al., 2004). In this context, the installation of special devices such as hydrodynamic separators can be a solution to protect receiving watercourses. Hydrodynamic separators are small structures currently used to capture large wastes and sediments. Several designs of hydrodynamic separators exist, each having its own operating process (Office of Water and US Environmental Protection Agency, 1999). The use of a solid/liquid separation mechanism along a screen allows the last generation of such devices to increase the efficiency of hydrodynamic separators (Andoh and Saul, 2003). The CycloneSep<sup>®</sup> works with these screening effects. The influent swirls and the screen retains debris and sediments on the external part of the device. After passing through the screen, the effluent is discharged in the environment (Figure 1). The efficiency of some hydrodynamic separators for trapping sediments has been investigated by experimental campaigns (Pathapati et al., 2009; Jefferies, 1998; Schmitt et al., 2012a). However, the mechanisms concerning the trapping efficiency of particles smaller than the aperture size of the screen is unexplored. Is it a simple sedimentation process or does the screen have an effective impact on the water/particle separation efficiency? In this context, a study coupling laboratory measurements and CFD modeling has been performed.

The aim of this article is to investigate a multiscale approach to study the efficiency of device hydrodynamic separator at the global and the local scale. The methodology consists in:

- studying and comparing the hydrodynamic characteristics with the particles trajectories,
- observing the influence of the particles characteristics in the trapping efficiency,
- assessing the influence of the screen shape in the local performance.

The long-term objective is to use this methodology to optimize the device and the shape of the screen and to conclude about the optimal configuration.

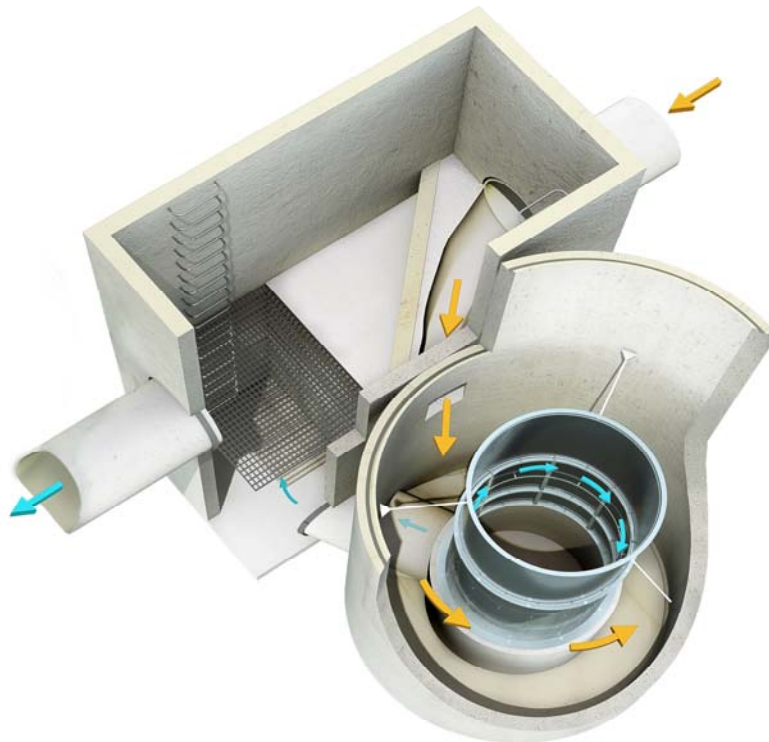


Figure 1: The hydrodynamic separator CycloneSep<sup>®</sup> (Hydroconcept)

## 2 METHODS

### 2.1 Multiscale CFD approach

#### 2.1.1 Fluid flow modelling

Currently, Computational Fluid Dynamics (CFD) is a powerful tool to investigate the hydraulic behaviour of hydraulic structures. It has been successfully used for storage tanks (Stovin et al., 1994; Adamsson et al., 2003; Dufresne et al., 2008; Lipeme Kouyi et al., 2010), lamella settlers (Vazquez et al., 2010) and hydrodynamic separators (Pathapati et al., 2009; Lee et al., 2010). The complexity of the geometry studied here (in particular the number and the shape of the apertures of the screen) requires the development of a multiscale method (Schmitt et al., 2012b). Therefore, two models are built (Figure 2).

##### *Small-scale model*

The aim of the first model is to reproduce the hydrodynamic phenomena that occur near the screen. The volume of the geometry was reduced to a portion of a cylinder (angle of 5°, radius of 0.5 m, height of 0.04m). The mesh was built with the *Cut-cell method* (Ansys, 2012) and is composed of 2,500,000 cells. The *non-equilibrium wall function* was used. This function is recommended for high three-dimensionality in the near wall region and severe pressure gradients in the boundary layer separations (Ansys, 2012). The turbulence RSM (Reynolds Stress Model) was used in order to take into account the effect of anisotropy of the turbulence on the velocity field. Concerning the boundary conditions, the tangential velocity measured near the screen was imposed as an inlet velocity (0,717 m/s corresponding to a discharge of 25 L/s (nominal discharge of the structure)). At the outlet, a negative velocity was selected to impose the discharge passing through the screen. This simulated discharge (0,042 L/s) is calculated proportionality to the global discharge (25 L/s). The intensity of turbulence (4.4 %) and the hydraulic diameter (0.04 m) are also considered in the simulation. Outflow conditions are applied on the inner surface in order to evacuate the water that goes through the screen. All other boundaries are considered as symmetry conditions.

The energy loss created by the screen is calculated with the following equation (Pernès, 2004):

$$\Delta H = \frac{\iint_{Inlet} \rho g \left( z + \frac{P}{\rho g} + \frac{V^2}{2g} \right) V_t dS - \iint_{Outlet} \rho g \left( z + \frac{P}{\rho g} + \frac{V^2}{2g} \right) V_t dS - \iint_{OutletScreen} \rho g \left( z + \frac{P}{\rho g} + \frac{V^2}{2g} \right) V_t dS}{\rho g Q} \quad (1)$$

with  $\Delta H$  the head loss,  $\rho$  the fluid density,  $g$  the gravity acceleration,  $z$  the altimetric position,  $P$  the pressure,  $V$  the velocity magnitude and  $V_t$  the tangential velocity.

##### *Global-scale model*

This energy loss was modeled at the global scale using a conceptual screen (and using a porous screen law). This method allows us to simulate the global hydrodynamic behaviour of the device without needing a detailed mesh near the screen (Schmitt et al., 2012b). Concerning the simulation, this approach introduces a source term that reproduces the energy loss of the screen; this model is relevant for high Reynolds numbers. This term is composed by the head loss coefficient  $K$ , the thickness  $\Delta m$ , the fluid density  $\rho$  and the velocity  $v$ .

$$S_i = - \left( \frac{K}{\Delta m} \frac{1}{2} \rho v^2 \right) \quad (2)$$

The multiphase *Volume of Fluid* model is chosen in order to reproduce the free surface position. Concerning the turbulence, the RSM model was suggested for swirling flows (Ansys, 2012). Concerning the boundary conditions, an inlet velocity sets the nominal discharge (25 L/s). The turbulent intensity and the hydraulic diameter are given too. A pressure condition at the outlet regulates the downstream water level (0.64 m). Atmospheric pressure is applied at the top of the volume. A grid sensitivity analysis allows us to conclude on the mesh discretization size. 1,200,000 cells are necessary for a sufficiently low numerical uncertainty.

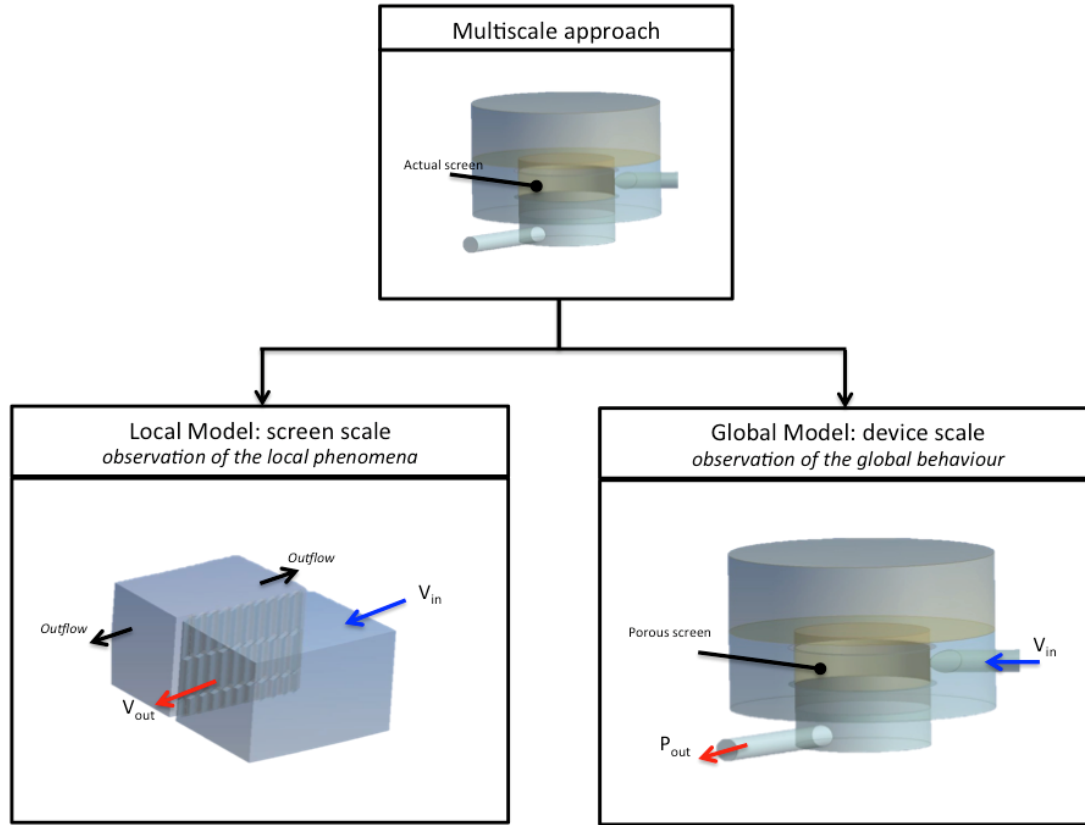


Figure 2: Multiscale approach: local model with the actual screen (left) and global model with the conceptual screen (right)

### 2.1.2 Particle trajectories modelling

The trapping efficiency of the device is evaluated with a Lagrangian approach. This method was used to visualize the particles trajectories in sedimentation tanks, basins (Stovin and Saul, 1998; Dufresne, 2009; Vosswinkel, 2012) and hydrodynamic separators (Egarr et al., 2004; Osei abs Andoh, 2008; Pathapati, 2009). In this approach, the particles trajectories are derived from Newton's second law and summarized by the following equations:

$$\frac{du_p}{dt} = F_D(u - u_p) + \frac{g_x(\rho_p - \rho)}{\rho_p} + F_x \quad (3)$$

with 
$$F_D = \frac{18\mu}{\rho_p d_p^2} \frac{C_D R_p}{24} \quad (4)$$

$$R_p = \frac{\rho d_p |u_p - u|}{\mu} \quad (5)$$

$$C_D = a_1 + \frac{a_2}{R_p} + \frac{a_3}{R_p^2} \quad (6)$$

$$C_D = \frac{24}{R_p} \quad (7)$$

Here  $u_p$  is the particle velocity;  $u$  the fluid velocity;  $\rho$  the fluid density;  $\rho_p$  the particle density;  $g_x$  the gravity  $x$  and  $F_x$  additional forces such as body forces and forces due to pressure gradients. The drag force  $F_D$  is composed of the water molecular viscosity  $\mu$ , the particle diameter  $d_p$ , the Reynolds number of the particle  $R_p$  and the drag coefficient  $C_D$ . The value of  $C_D$  is depending on the flow regime. For small Reynolds number ( $R_p < 0.1$ ), the drag coefficient is calculated with the equation (7); for  $0.1 < R_p < 1000$  with equation (6); and is equal to a constant equal to 0.4 for  $R_p > 1000$ . Concerning the

interaction with walls, the reflect condition is imposed. The particles that hit the walls will be therefore reflected in the flow.

At first, the multiscale approach is used to observe the particle trajectories in the device. Because of the simplification of the screen, the global model cannot be used to calculate the device efficiency. The porous wall is used to reproduce the hydrodynamic behaviour and can not model the collision between the particle and the solid part of the screen. An *interior* condition is used for the porous wall to ensure the continuity of the particle trajectory downstream the screen. However, this model will be used to visualize the influence of the particles characteristics (density and diameter) on the sedimentation process and to determine what kind of particle can potentially pass through the screen. A comparison with the hydrodynamic behaviour is made to find a link with the particles trajectories. Three diameters are studied (500, 1000 and 1500  $\mu\text{m}$ ) for various densities (1040 to 2600  $\text{kg/m}^3$ ). These values correspond to a range representing particles of a rainwater sewer system. The efficiency at the global scale is calculated by making a mass balance between the particles that are injected and the particles trapped by the separator:

$$GE (\%) = \text{Particles retained} / \text{Particles injected} \times 100 \quad (8)$$

The local model is used to estimate qualitatively the influence of the shape of the screen. Indeed, only a portion is modelled and the screen efficiency does not correspond to the device efficiency. A comparison between two types of screens (expanded metal vs perforated plate) enables us to observe the influence of the shape on the efficiency. The visualization of the turbulent kinetic energy and of the particle trajectories shows the influence of the local hydrodynamic effects. Different characteristics of particles are investigated: four diameters (35, 500, 1200 et 1500  $\mu\text{m}$ ) and four densities (1040, 1200, 1700 et 2500  $\text{kg/m}^3$ ). The screen efficiency is calculated as follows:

$$SE (\%) = \text{Particles retained} / \text{Particles injected} \times 100 \quad (9)$$

## 2.2 Experiments

The experimental pilot is mainly used to validate the numerical method (Figure 3). The dimensions of the pilot are similar to real-life devices that are installed in small catchment areas. The device is 1 m high and the external diameter is equal to 2 m. The screen has a diameter of 1 m and a height of 0.33 m. The dimensions of the apertures are as follow: 17 mm x 1.65 mm and the angle of the metal stripe is 60°. The screen is located from  $z = 0.22$  m to 0.55 m. The diameters of the inlet and outlet pipes (respectively located at  $z = 0.55$  m and  $z = -0.2$  m) are equal to 200 mm. The two pipes are equipped with butterfly valve in order to respectively regulate the discharge and the water level in the pilot.

An electromagnetic flowmeter measures the discharge in the inlet pipe (relative uncertainty of +/- 1% of the measurement). An Acoustic Doppler Velocimeter (ADV) is used to measure the velocity and the turbulence fields (relative uncertainty of +/- 1% of the measurements). Twelve radial and four horizontal planes located around the screen are used to map the hydrodynamic behaviour. The water level is measured with two ultrasonic sensors (+/- 1 mm).

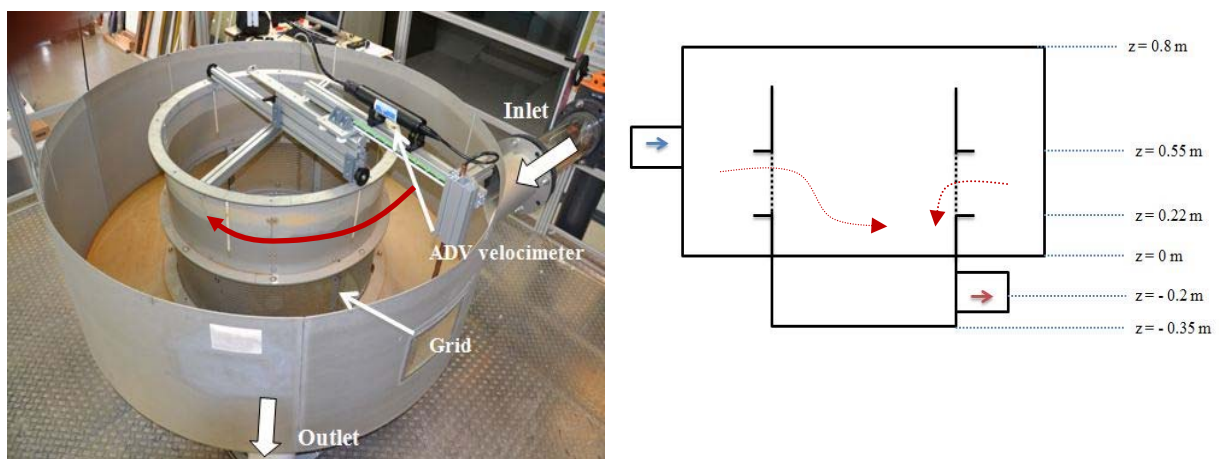


Figure 3: Experimental setup of the CycloneSep®



### 3 RESULTS

#### 3.1 Global scale investigations

From a hydrodynamic point of view, the comparison between experiments and modeling allows us to validate the global model of our approach. By comparing the horizontal velocity fields, we observe that the model reproduces the velocity profile (Figure 4). The fact that a porous wall conceptually models the screen is probably responsible for the local differences nearby the screen (mean error of 15% (Schmitt et al., 2012b)). However, the results are sufficiently good to draw some conclusions about the particle trajectories in the device.

Figure 5 shows the influence of the particle density and the particle diameter. The device traps all particles higher than 500  $\mu\text{m}$  and 2600  $\text{kg}/\text{m}^3$  for a flow rate equal to 25 L/s. By observing the graph, we can suppose that particles with low diameters and low densities are potentially steered by the hydraulic behaviour: 100% of the particles lower than 1040  $\text{kg}/\text{m}^3$  pass through the conceptual screen.

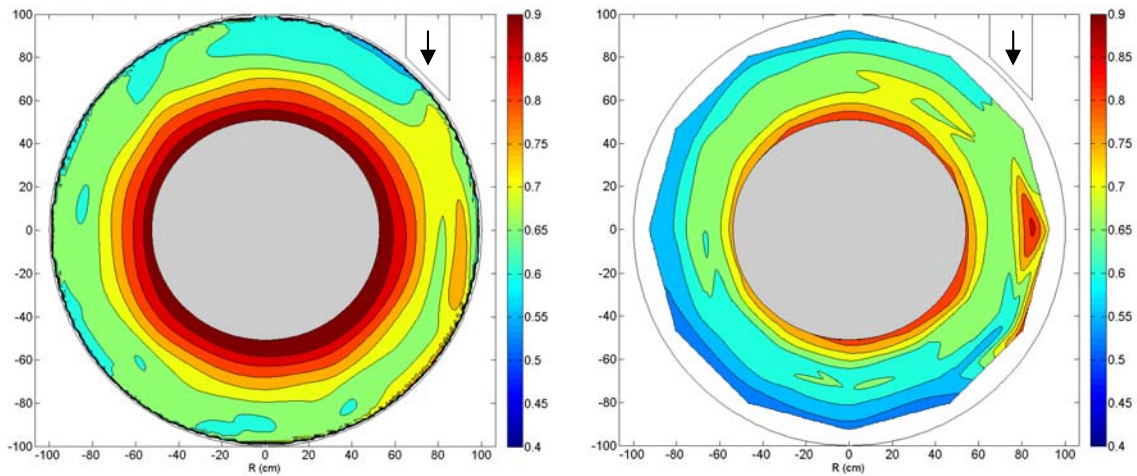


Figure 4: Horizontal velocity field ( $z = 38 \text{ cm}$ ) obtained with the CFD global model (left) and the experiment (right) for a nominal flow rate equal to 25 L/s

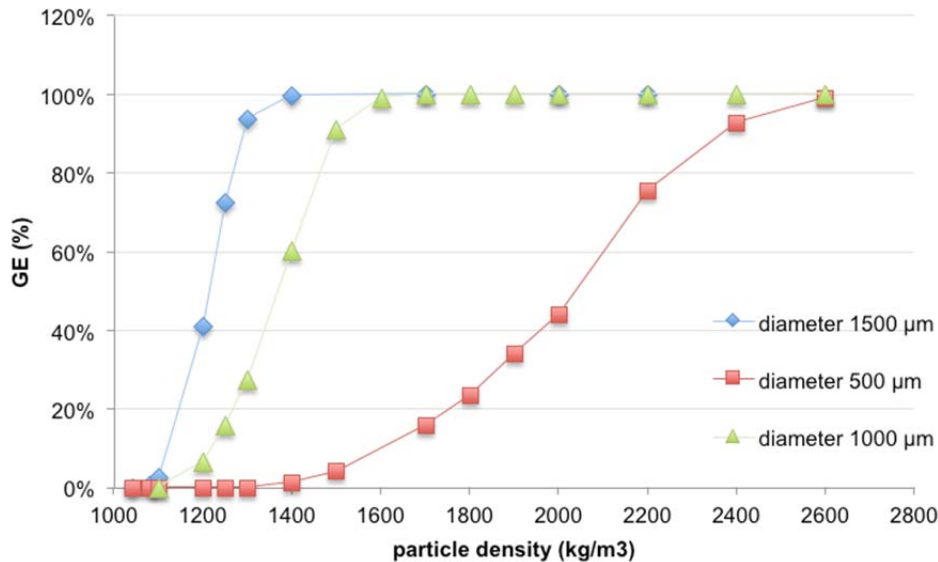
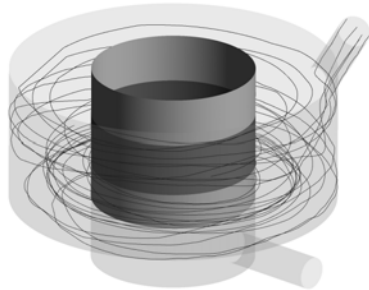


Figure 5: Particles tapping efficiency with the conceptual porous screen ( $Q = 25 \text{ L/s}$ ) for different particles characteristics

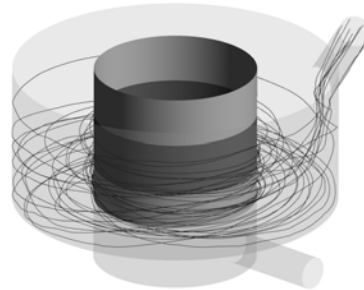
To explain the previous results, we have drawn the trajectories of ten particles with various characteristics (Figure 6). A greater density is responsible for a quick sedimentation of the particle. For the characteristics 4, particles are directly on the bed of the device and turn around the central plate.

On the contrary, the distribution of particles with small densities (characteristics 1 and 2) is mainly controlled by the mean flow. Particles are swirling around the screen approximately 8 times before passing through the porous screen. This behavior is relevant with the residence time of a fluid particle (Schmitt et al., 2012b). This confirms the fact that particles with low densities are steered by the hydrodynamic behaviour.

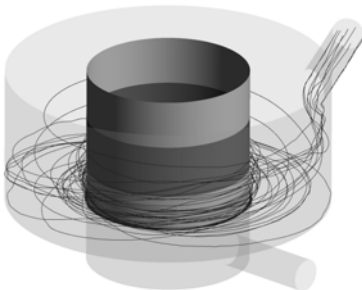
*characteristics 1:*  $\rho = 1040 \text{ kg/m}^3$   $d = 500 \text{ }\mu\text{m}$



*characteristics 2:*  $\rho = 1040 \text{ kg/m}^3$   $d = 1500 \text{ }\mu\text{m}$



*characteristics 3:*  $\rho = 1700 \text{ kg/m}^3$   $d = 500 \text{ }\mu\text{m}$



*characteristics 4:*  $\rho = 1700 \text{ kg/m}^3$   $d = 1500 \text{ }\mu\text{m}$

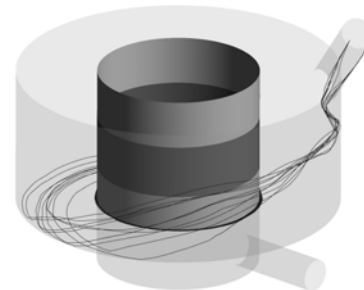


Figure 6: Trajectories of 10 particles in the pilot using a conceptual porous screen for a flow rate equal to 25 L/s

### 3.2 Screen efficiency

The simulated fluid flow allows us to observe the impact of the screen shape. By increasing the angle of the metal stripe and decreasing the aperture size, the pressure and the turbulent kinetic energy gradients increase, which probably favor the ejection of particles. These phenomena are clearly illustrated on Figure 7. A zone with high turbulence ( $0.035 \text{ m}^2/\text{s}^2$ ) is present in the opening of the "expanded metal" screen. For the perforated plate, the turbulence zone is present downstream of the screen. Upstream of the screen, the turbulent kinetic energy is equal to  $0.005 \text{ m}^2/\text{s}^2$ .

The particle tracking enables us to visualize the efficiency of a screen by comparing the two screens. The results are shown on Table 1. For the same hydraulic conditions, the "expanded metal" screen retains about 140% more particles than the perforated plate. This assessment is increased for small particles with low densities.

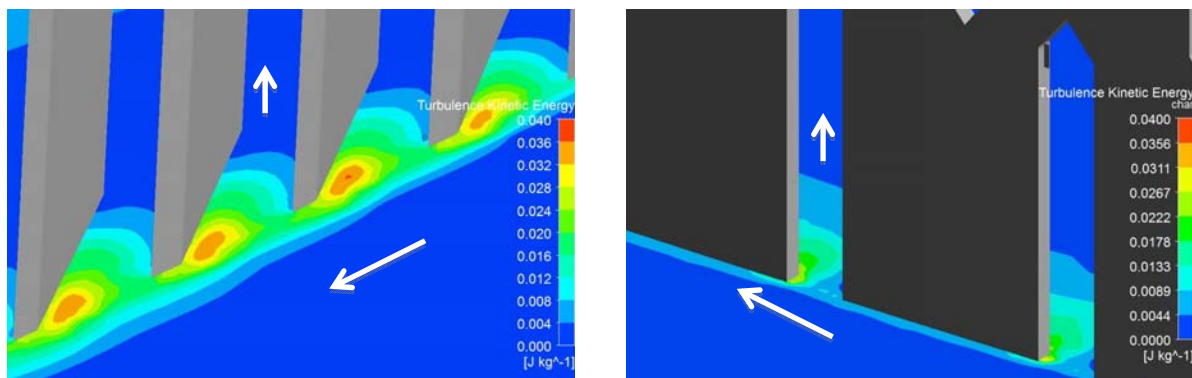


Figure 7: Turbulent kinetic energy field for two different screens for an equivalent flow rate of 25 L/s: expanded metal screen (left) and perforated plate with hexagonal (right)

Table 1: Screen efficiency of "expanded metal screen" compared to the one of a perforated plate.

Density	d=1200 $\mu\text{m}$			d=35 $\mu\text{m}$		
	SE expanded metal (%)	SE perforated plate (%)	SE expanded metal/SE perforated plate (%)	SE expanded metal (%)	SE perforated plate (%)	SE expanded metal/SE perforated plate (%)
$\rho = 1200 \text{ kg/m}^3$	86	50	172	65	46	141
$\rho = 1700 \text{ kg/m}^3$	98	64	166	65	46	141
$\rho = 2500 \text{ kg/m}^3$	100	71	141	65	47	138

To explain the efficiency of the expanded metal screen, we have drawn the particle trajectories with various densities. The illustrations on Figure 8 demonstrate that the heaviest particles are ejected outside (Figure 8 d). For small densities (Figure 8 a), we can observe the separation of the trajectories. Particles that pass through the screen are separated before the high turbulence zone ( $0.03 \text{ m}^2/\text{s}^2$ ). The explanation is probably the inertia of the particles. For low densities, the trajectories of the particles are easily modified. On the contrary, the trajectories of for heavy particles are more difficult to modify.

The link between the turbulent kinetic energy, the particle tracking and the local efficiency will be the object of a further work.

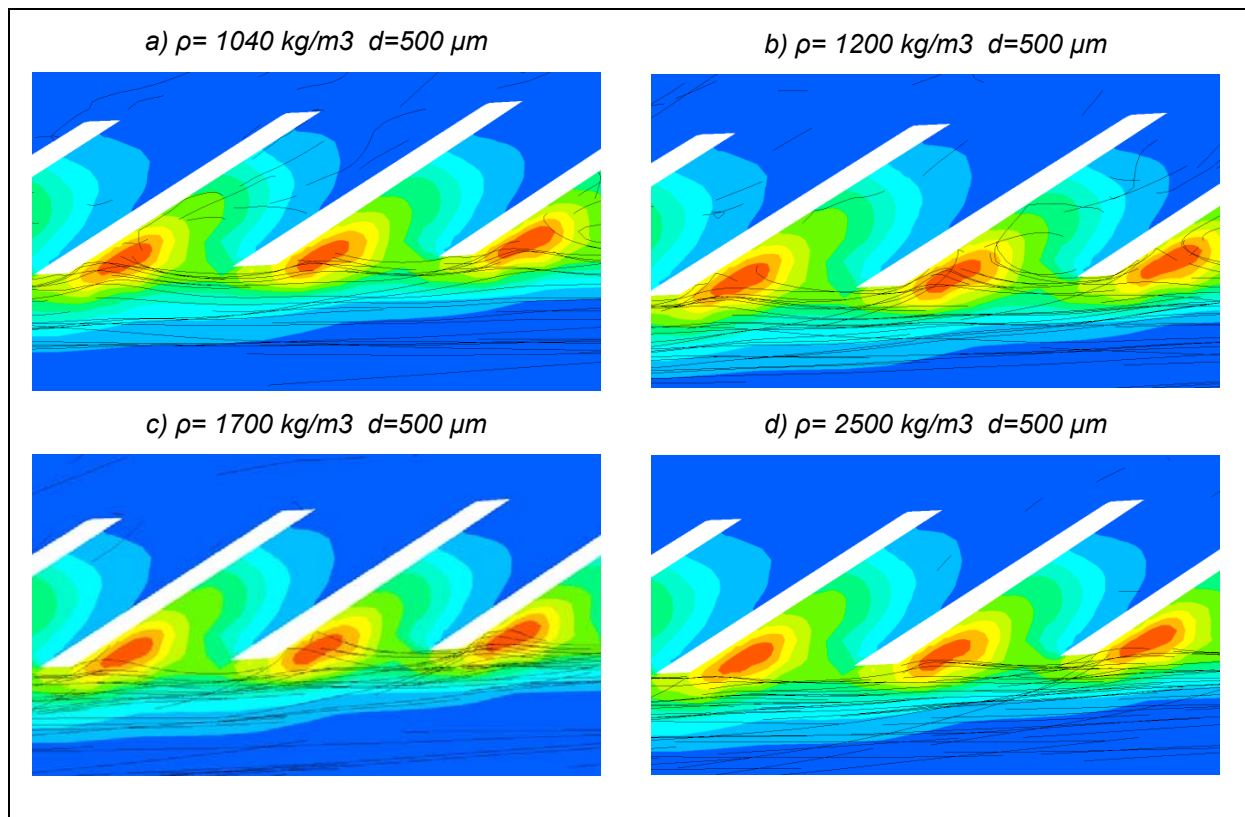


Figure 8: Turbulent kinetic energy field and particles trajectories with different characteristics for an equivalent flow rate equal to 25 L/s



## 4 CONCLUSION

The objective of the study was to investigate the use a CFD multiscale approach to visualize and explain the various hydrodynamic phenomena that occur in a hydrodynamic separator at different scales. A local model representing a portion of the screen was used to study the local phenomena that occur nearby the screen. A global model reproduced the global behaviour of the device. A porous wall (screen simplification) was calibrated to simulate the energy loss created by the actual screen. The solid/liquid efficiency was predicted using a Lagrangian particle tracking at the two scales.

The global behaviour showed that the trapping efficiency of the device is function of the particles characteristics. The hydrodynamic separator traps heavy particles by sedimentation process. Results obtained with the numerical method showed that the particles with small densities are steered by the hydrodynamic behaviour. This kind of particles can only be retained by the local phenomena produced by the screen.

The local model enabled us to observe the influence of the screen shape. The comparison between two types of screens allowed us to visualize the effect of the turbulent kinetic energy in the solid separation prevision. A higher turbulent zone favours the ejection of particles. The inertia process can explain the fact that particles with low densities are more sensitive.

To conclude, the use of a CFD multiscale approach and particle tracking is relevant for predicting solid separation along a screen. The long-term objective is to use this methodology for the device optimization (favour the deposits region, avoid the resuspension of sediments) but also the screen shape (increase the turbulent kinetic energy field and the pressure effects).

## ACKNOWLEDGEMENT

We would like to acknowledge the firm Steinhardt Wassertechnik for the construction of the pilot, Ile de France Innovation and the GEMCEA for its financial support. I also would like to acknowledge the HPC centre of the University of Strasbourg for the computational clustering support.

## LIST OF REFERENCES

- Adamsson, Å., Stovin, V.R. & Saul, A.J. (2003). *Bed shear stress boundary condition for storage tank sedimentation*. Journal of Environmental Engineering, 129(7), 651-658.
- Andoh, R.Y.G & Saul, A.J. (2003). *The use of hydrodynamic vortex separators and screening systems to improve water quality*. Water Science and Technology, 47(4), 175-183.
- Ansys, (2011). Fluent 14.0 User's Guide. Ansys Inc.
- Ashley, R.M., Bertrand-Krajewski, J.L. & Hvited-Jacobsen, T. (2004). *Solids in sewers*. IWA publishing, Scientific and technical report n°14.
- Chebbo, G. (1992). *Solides des rejets urbains par temps de pluie : caractérisation et traitabilité*. Thèse de doctorat, Ecole nationale des ponts et chaussées, Paris, France.
- Chocat, B. (1997). *Encyclopédie de l'hydrologie urbaine et de l'assainissement*, Bassins de retenue p. 95, Eurydice 92, Ed Tec&Doc Lavoisier, Paris, 1997, 1121 p.
- Dufresne, M., Vazquez, J., Terfous, A., Ghenaim, A. & Poulet, J.B. (2009). *Experimental investigation and CFD modelling of flow, sedimentation, and solids separation in a combined sewer detention tank*. Computers & Fluids 38(5), 042-1049.
- Egarr, D.A., Faram, M.G., O'doherty, T., Syred, N., (2004) *AN investigation into factors that determine the efficiency of a hydrodynamic vortex separator*. 5th International Conference on Innovative Technologies in Urban Storm Drainage, Novatech '04, Lyon, France.
- Jefferies, C., Allinson, C.L., McKeown, J. (1998) *The performance of a novel combined sewer overflow with perforated conical screen*. Water Science and Technology, 37(1), 243-250.
- Lee J.H., Bang K.W., Choi C.S., Lim H.S. (2010). *CFD modelling of flow field and particle tracking in a hydrodynamic stormwater separator*. Water Science and Technology, 62 (10).
- Lipeme-Kouyi, G., Arias, L., Barraud, S., Bertrand-Krajewski, J-L., (2010) *CFD Modelling of flow in a large stormwater detention and settling basin*. 7th International Conference on Innovative Technologies in Urban Storm Drainage, Novatech '10, Lyon, France.
- Office of Water and US Environmental Protection Agency. (1999). *Stormwater Technology fact sheet hydrodynamic separator*.
- Osei, K. & Andoh, R., (2008) *Optimal grit and control in collection systems and at treatment plants*. World

- Environmental & Water Resources Congress. May 12-16, 2008, Honolulu, Hawaii
- Pernès, P. (2004). *Hydraulique unidimensionnelle: Partie 1 et 2*. Cemagref editions
- Pathapati S.S and Sansalone J.J., (2009). *CFD modeling of a storm-water hydrodynamic separator*. Journal of Environmental Engineering. 135(4), 191-202.
- Stovin, V.R. & Saul, A.J. (1994). *Sedimentation in storage tank structures*. Water Science and Technology, 29(1-2), 363-372.
- Stovin, V.R. & Saul, A.J. (1998). *A computational fluid dynamics (CFD) particle tracking approach to efficiency prediction*. Water Science and Technology, 37(1), 285-293.
- Schmitt, V., Dufresne, M., Vazquez, J., Fischer, M., Morin, A. (2012a) *Etude expérimentale et numérique du CycloneSep*, Rapport de convention d'étude pour la société Hydroconcept.
- Schmitt, V., Dufresne, M., Vazquez, J., Fischer, M., Morin, A. (2012b) *Optimization of a hydrodynamic separator using a multi-scale computational fluid dynamics approach*. 9th International Conference on Urban Drainage Modelling. Belgrade, Serbie.
- Vazquez, J., Morin, A., Dufresne, M., Wertel, J., (2010) *Optimisation de la forme des décanteurs lamellaires par la modélisation hydrodynamique 3D*. 7th International Conference on Innovative Technologies in Urban Storm Drainage, Novatech '10, Lyon, France.
- Vosswinkel, N., Schnieders, A., Maus, C., Ebbert, S., Mohn, R., Uhl, M., (2012) *Comparison of flow and sedimentation pattern for three designs of storm water tanks by numerical modelling (CFD)*. 9th International Conference on Urban Drainage Modelling. Belgrade, Serbie.